Structural and Morphological Changes during UV Irradiation of the Crystalline Helical Form of Syndiotactic Polypropylene

Liberata Guadagno,* Carlo Naddeo, and Vittoria Vittoria

Dipartimento di Ingegneria Chimica e Alimentare Università di Salerno, Via Ponte Don Melillo 1, 84084 Fisciano, Salerno, Italy

Received August 5, 2004

ABSTRACT: Syndiotactic polypropylene films, in the most usual crystallographic modification (form I), were exposed to accelerated weathering in a UV device at 45 °C for increasing times. A different series of films characterized by the same structural organization were annealed at 45 °C to discern the thermal effects from those due to UV irradiation. The influence of UV irradiation and thermal treatments on the structural changes in terms of phase composition, crystallite sizes, and chain conformations was investigated. The analyzed samples were crystallized from the melt at 25 °C, obtaining the disordered crystalline form I, with chains in helical conformations, in large amounts, and a small fraction of mesophase with chains in trans-planar conformations. Diffractometric and thermal analysis have shown that UV radiation causes a strong increase in the crystallinity degree within the first 170 h of treatment. Such an increase mainly occurs by an increase in the coherent crystalline domain size in the direction perpendicular to the (200) planes. Spectroscopic data (FTIR) confirm that the increase in the crystallinity degree occurs not only by a strong reduction of the amorphous phase and a consistent increase of the conformational order of the chains in helical conformation but also by a reduction of the domains with chains in the trans-planar conformation. The trans-planar domains, very small and arranged in the amorphous matrix, are attached by UV radiation together with the amorphous phase. The observed phenomena are to be attributed to the effects of chain scission due to the photooxidation. Samples only annealed at 45 °C show only small effects of physical aging within the first 10 h of treatment.

Introduction

The recent use of metallocene catalysts for producing polypropylenes has allowed getting a new syndiotactic polypropylene with high stereoregularity and interesting mechanical properties.[1−3] Among these, a peculiar property has been found: samples of oriented syndiotactic polypropylene show a very interesting elasticity similar to that shown by thermoplastic elastomers. In addition, these samples offer great advantages if compared to conventional elastomers for their higher values of modulus.[4−8]

The initial research on sPP focused on the physical−chemical characteristics of the material. Indeed, complex aspects of polymorphism displayed by this polymer were clarified.

Four crystalline forms of sPP have been described so far. Forms I and II are characterized by chains in the $(T_2G_2)_n$ helical conformation,[9−10] whereas forms III and IV present chains in trans-planar and $(T_6G_2T_2G_2)_n$ conformations,[11,12] respectively. Form I is the stable form of sPP, obtained under the most common crystallization conditions either from the melt or from solution as single crystals.[9,13−16] Different kinds and amounts of disorder of the crystalline phase, depending on the degree of stereoregularity and the mechanical and thermal history, were described in rapidly crystallized samples.[16] In specimens quenched from the melt in a cold bath at 0 °C for many days, the presence of form III[17] or of a trans-planar mesophase[18] was recognized. Stretching either the helical form I or the trans-planar mesophase, the crystalline form III with the chains in trans-planar conformation is obtained when the sample is fixed at λ around 6−7, whereas the starting conformations again form when the tension on the sample is relaxed.[6,7,19]

Current studies on sPP look at the problems of application. Yoshino and others[20,21] have highlighted another important characteristic of this novel sPP, that is, its electrical properties which are superior to those of iPP. This effect translates into higher resistance to pulse breakdown with respect to iPP.[22] This characteristic, combined with a much higher resistance to impact than that of iPP, makes sPP particularly suitable for insulation in electrical machinery. Kohalmy and others[22] have shown that sPP is particularly appropriate also in the manufacturing of insulating cables for electrical wiring and therefore could be used to substitute conventional cross-linked polyethylene (XLPE), which requires complex cross-linking using peroxide for successful welding.

For these potential and specific sPP applications, the degradation studies are of topical and international interest. In this work, we have analyzed the photooxidative durability of sPP films in the crystalline stable helical form.

The photooxidative degradation is carried out by exposing film to UV-A radiation, reproducing the ultraviolet component of solar radiation which strikes the earth's surface (295−380 nm). This radiative treatment has been realized in the presence of oxygen and humidity. The research has allowed understanding the structural and morphological changes connected to the photooxidation phenomena.

Experimental Section

Materials. Syndiotactic polypropylene (sPP) pellets formulated without slip and antiblock were bought from the Aldrich Polymer Products. The polymer density, molecular weight, and

* Corresponding author: e-mail lguadagno@unisa.it; fax +39 089 964057.

10.1021/ma040129j CCC: $27.50
Published on Web 12/04/2004

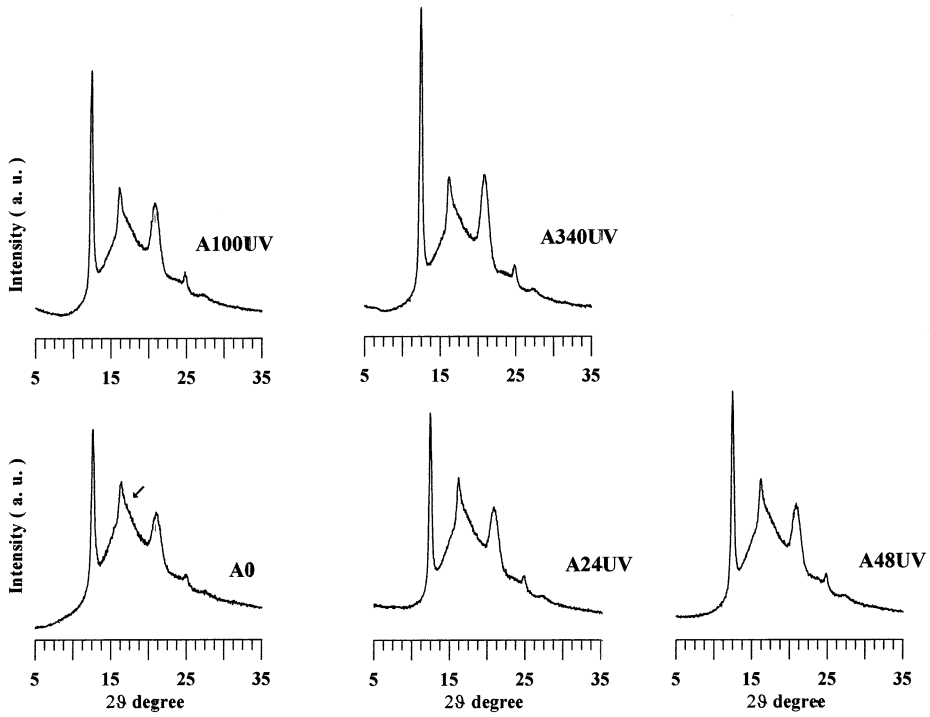

Figure 1. X-ray diffractograms of sample A0 exposed at increasing UV irradiation times (0, 24, 48, 100, 340 h).

melt index were respectively 0.900 g/mL, 127 000, and 4.5 g/10 min (ASTM 1238).

The polymer was analyzed by ^{13}C NMR spectroscopy at 120 °C on a Bruker AM 250 spectrometer operating in the FT mode at 62.89 MHz, by dissolving 30 mg of sample in 0.5 mL of $C_2D_2Cl_4$. Hexamethyldisiloxane was used as internal chemical shift reference. Our sample showed 89% syndiotactic pentads.

sPP pellets were molded in a hot press (Carver Inc.), at 170 °C, forming 70 ± 5 μm thick films, which were rapidly quenched in a bath at room temperature (samples A0). Some of them were UV irradiated, for different times, in a accelerated photoageing device Q-Panels (model QUV/spray) equipped with medium-pressure mercury lamps at temperature of 45 °C, which the glass envelope filters out light with $\lambda < 290$ nm. The UV irradiance times were 1 h (A1UV), 2 h (A2UV), 3 h (A3UV), 6 h (A6UV), 10 h (A10UV), 24 h (A24UV), 33 (A33UV), 48 h (A48UV), 100 h (A100UV), 170 h (A170UV), 200 h (A200UV), 250 h (A250UV), and 340 h (A340UV). Others samples were subjected for the same times only at thermal treatment of 45 °C (sample AtT, where t is the time in hours as in the lines back).

Methods. Wide-angle X-ray patterns (WAXD) were obtained using a Philips PW 1710 powder diffractometer (Cu Kα Ni-filtered radiation) with a scan rate of 1°(θ)/min.

Differential scanning calorimetry (DSC) was carried out using a thermal analyzer Mettler DSC 822/400 equipped with DSC cell purged with nitrogen and chilled with liquid nitrogen for subambient measurements. The temperature range was −50 °C/250 °C at a heating rate of 20 °C/min.

The infrared spectra were obtained in absorbance mode using a Bruker IFS66 FTIR spectrophotometer with a 2 cm^{-1} resolution (64 scans collected). The absorbances of the trans-planar conformational bands at 831, 963, and 1132 cm^{-1} and of the helical bands at 810, 977, and 1005 cm^{-1} were normalized with the absorbance of the band at 2724 cm^{-1}. All the bands which result to be composed from different vibrational modes were decomposed into the different components, using a complex fitting in which a Lorentzian and a Gaussian contribution were considered in the form

$$f(x) = (1 - L)H \exp\left[-\left(\frac{x - x_0}{w}\right)^2 (4 \ln 2)\right] + L \frac{H}{4\left(\frac{x - x_0}{w}\right)^2 + 1}$$

where x_0 is the peak position, H is the height, w is the width at half-height, and L is the Lorentzian component.

Results and Discussion

Structure of the Initial and Irradiated Samples. In Figure 1, together with the X-ray diffraction pattern of the starting sample (A0), we show the patterns of sample A0 at increasing times of UV irradiation (24, 48, 100, and 340 h). The X-ray diffractogram of A0 sample indicates that the sample crystallized in the usual form I, characterized by the most intense peaks at 12.3° (200 reflection), 15.9° (010 reflection), and 20.8° of 2θ, corresponding to the 210 reflection. In the diffractogram the weak reflection at $2\theta = 24.8°$ corresponding to the 400 reflection is also evident. The absence of the 211 reflection at $2\theta = 18.8°$ is a clear indication that we obtained the disordered form I as expected for a sample crystallized at low temperatures. In fact, the preferential crystallization of the disordered form was always found in samples of low syndiotacticity or in powder samples crystallized from the melt at temperatures below 120 °C.[6,10,19] In this case, departures from the fully regular alternation of helices of opposed chirality along both a and b axes were proposed. Though characteristic of the disordered form I, characterized by chains in helical conformation; the spectrum shows a small shoulder at 17° of 2θ (see arrow in Figure 1) typical of the mesophase with chains in the trans-planar conformation.[7,18] It was previously shown that the trans-planar mesophase can be formed keeping the sample for a long time at 0 °C, but it can be obtained, although as a minor fraction, also at 25 °C.[8] The X-ray diffractogram of sample A0 reveals therefore the presence of a small fraction of trans-planar mesophase. The presence of small mesomorphic domains, with chains in trans-planar conformation, will be put also in evidence too by FT/IR analysis.

With regard to the structure of the irradiated samples, we can note that the diffractometric profile of each sample shows the above-mentioned four reflections,

Table 1. Crystallinity, X_C (%), and Crystallite Coherence Lengths Perpendicular to Reflection Planes 200 (D_{200}) and 010 (D_{010}) Derived from X-ray Diffraction Measurements (Estimated Error Bars Are Supplied)

sample	time (h)	X_C (%)	D_{200} (Å)	D_{010} (Å)
A0	0	17 ± 1	341 ± 12	319 ± 10
A24UV	24	21 ± 2	394 ± 14	320 ± 10
A48UV	48	27 ± 2	394 ± 14	319 ± 10
A100UV	100	32 ± 2	403 ± 14	320 ± 10
A200UV	200	37 ± 2	428 ± 15	321 ± 10
A340UV	340	40 ± 2	377 ± 13	319 ± 10
A24T	24	18 ± 1	341 ± 12	320 ± 10
A48T	48	18 ± 1	340 ± 12	320 ± 10
A100T	100	19 ± 1	342 ± 12	321 ± 10
A200T	200	18 ± 1	341 ± 12	320 ± 10
A340T	340	19 ± 1	342 ± 12	319 ± 10

denoting that the crystallographic modification does not undergo any change under the influence of UV radiation. An accurate observation of the diffractograms allows us to observe that, on increasing of the irradiation time, the peak at $2\theta = 15.9°$ becomes more and more symmetric, as a consequence of the decrease in intensity of the shoulder at $2\theta = 17°$. It is clear that the radiative treatment reduces the fraction of transplanar mesophase. Furthermore, we observe that the radiation causes a strong increase in the crystallinity degree. In fact, from the profile of the patterns, it can be observed that the intensity of the peaks at 12.3° and 20.8° of 2θ very much increases with the irradiation time. In addition, the half-height width decreases, indicating a progressive improvement of the crystal dimensions. Using the pattern of atactic polypropylene to quantify the noncrystalline component, it has been derived an approximate crystallinity value for all the samples by comparing the area of the crystalline peaks with the total area, that is $X_C = (A_C/A_{TOT}) \times 100$ as reported in the literature.[23] In these calculations, to estimate the crystallinity of the helical form I from the diffractogram, the atactic background was subtracted and the crystalline peaks were decomposed into the single peaks at 12.3, 15.9, 17, and 20.8 of 2θ following a procedure already reported in the literature.[24] The obtained values are reported in Table 1. We can observe that, increasing the irradiation time, the films undergo a progressive increase of the crystallinity degree. The greatest crystallinity value is found in the sample A340UV, for which an increase of 135% is observed with respect to the starting sample A0. As mentioned before, wide-angle X-ray diffractograms were obtained on samples exposed either to UV radiation or to a temperature of 45 °C in order to differentiate the effects due to the radiation respect to those deriving by the only increase of temperature. In Figure 2, the diffractogram of the initial sample A0 is put together with diffractograms of the samples kept at 45 °C for increasing times (100 and 340 h). Crystallinity values have also been evaluated for these samples and are reported in Table 1. From these data, it is evident that the remarkable and progressive increase of the crystallinity degree shown by the irradiated samples does not occur in samples exposed only to the heat treatment. In fact, we observe an almost constant value of the crystallinity degree, and therefore the increase in crystallinity degree is due to the UV radiation and not to the effects of the annealing treatment.

From the diffractometric profiles, we derived the crystallite dimensions using the Scherrer equation:[25]

$$D = \frac{K\lambda}{\beta \cos \vartheta}$$

where D is the crystallite size, λ is the wavelength of the employed X-rays, ϑ is the diffraction angle, β is the half-height width, and K is a constant generally assumed as 0.9. The results are also reported in Table 1 for the values of D_{200}, the coherent crystalline domain size in the direction perpendicular to the (200) planes, and of D_{010}, perpendicular to the (010) planes, obtained respectively from the full width at half-height of the 200 and 010 profiles. The data reported in Table 1 do not show any appreciable variation in the crystallite sizes for the samples annealed at 45 °C, unlike what we observe for irradiated samples. In fact, the increase of crystallinity in the irradiated samples occurs with a simultaneous and strong increase in the crystallite coherence lengths perpendicular to the (200) planes. At variance we do not find any appreciable change for the (010) planes with respect to the initial value of 319 Å. The latter result points to a different ability, in the two crystallographic directions, of lamellar crystals of sPP helical modifications to host defects during the crystallization process induced by UV radiation. The D_{200} parameter increases of 26% after 200 h of irradiative treatment. For 340 h of treatment, we can observe a slight decrease of the D_{200} parameter. This reversal trend can be explained considering that, for extended times of exposure, the progression of the degradative phenomena has reached an advanced stage. Most probably, the degradation is extended up to the crystallites surfaces conditioning their dimensional stability. In fact, a scission of chains, on the crystallite boundary surfaces, disturbing the order of molecular segments adjacent to the crystals determines a reduction of their dimensions. This interpretation is also confirmed by the lowest value of the melting temperature observed in the calorimetric trace of the A340UV sample (see later). From the diffractometric data, we reach the conclusion that the UV radiation leads to a decrease of the mesophase fraction and to an increase of crystallinity. It is well-known that the polymer photooxidation is accompained by degradation that is the result of the decomposition

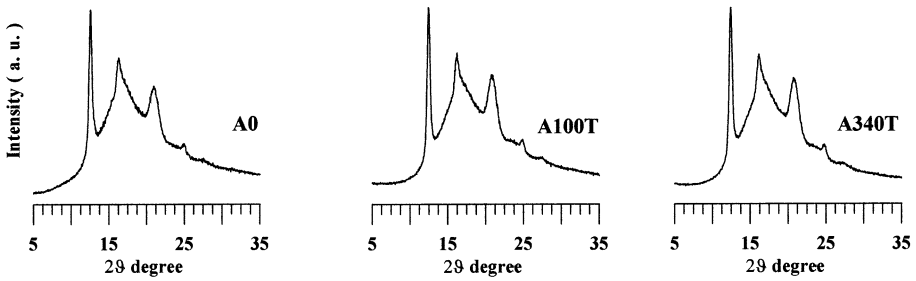

Figure 2. X-ray diffractograms of samples annealed at 45 °C for increasing times (0, 100, 340 h).

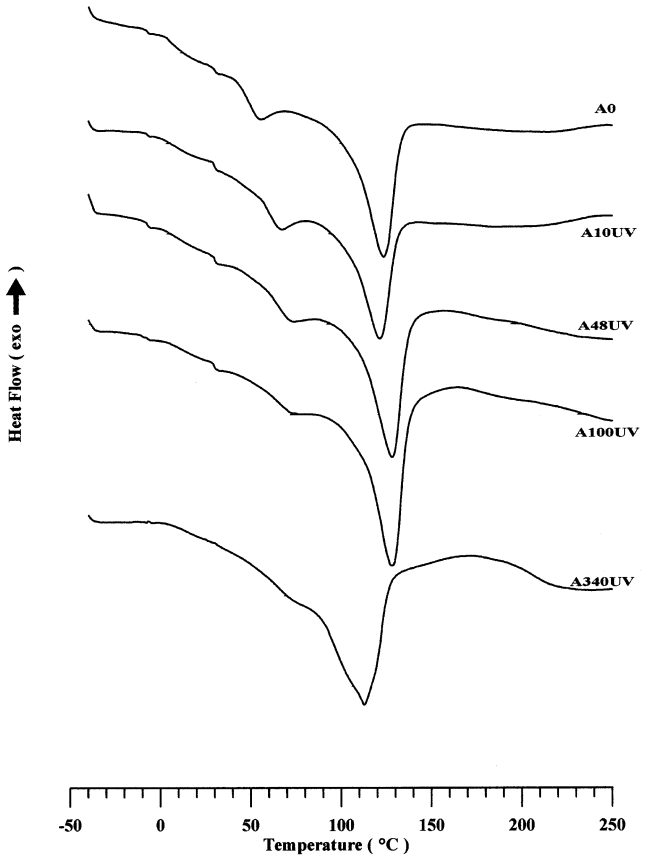

Figure 3. Thermograms of samples exposed at increasing UV irradiation times (0, 10, 48, 100, 340 h).

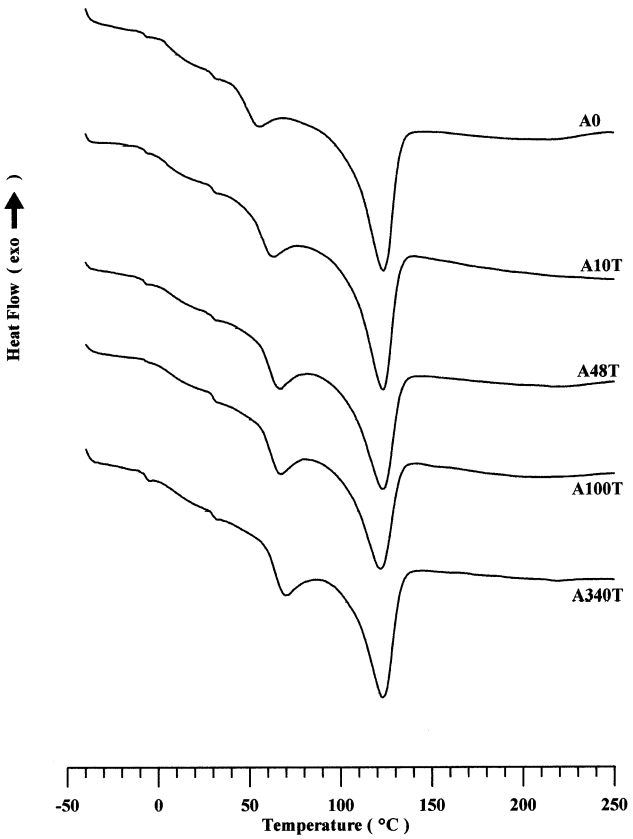

Figure 4. Thermograms of samples annealed at 45 °C for increasing times (0, 10, 48, 100, 340 h).

of macroradicals with the C−C bond scission. The chain scission makes the shortest chains in the amorphous phase more mobile and free to crystallize further in the more stable form I crystals. This effect, beside increasing the crystallinity, also favors the growth of preexisting crystal dimensions. In our case, the increase of the crystallinity degree does not occur through a continuous growth of the crystallite sizes; when the degradation is extended (as shown later by FT/IR analysis) and the virgin amorphous phase is extremely reduced, the sequence in the repetitive constitutional unit along the chains interrupts, preventing the growth on preexisting crystals. For this reason, the increase in the crystallinity occurs only in those small regions of the virgin amorphous phase, where the sequence in the repetitive constitutional unit along the chain is not interrupted by the photooxidation products, which are attached to the polymeric chain.

Differential Scanning Calorimetry (DSC). In Figure 3, we report some thermograms of samples exposed to increasing UV irradiation times. In the starting sample A0, at low temperature, we observe a pronounced deflection of the baseline in the −10 to 10 °C range, due to the glass transition, followed by a first small endothermic peak centered at 53 °C. For the sPP samples, this endothermic peak was associated with the melting or disordering of the trans-planar mesophase,[7,26,27] which transforms into the helical crystalline form at temperatures higher than 60 °C.[28−32] The endothermic peak, centered at about 137 °C, corresponds to the usual melting temperature of the sPP in form I. We can note that the first endothermic peak progressively reduces and shifts at higher temperature as the degradation goes on.

In Figure 4, we report the thermograms of films annealed at 45 °C for increasing times. We can note that, also in this case, the first endotherm shifts at higher temperatures on increasing the permanence at 45 °C. However, unlike the irradiated samples, no decrease is noted in the entity of this peak on increasing the time. We can conclude that the shift at higher temperatures is due to the permanence at 45 °C in both cases. In fact, the permanence at 45 °C determines an improvement in the chains packing of the trans-planar mesophase domains and accordingly a higher melting temperature. As for the decrease of enthalpic content, which is only observed in the irradiated samples, it is evident that the radiation UV causes a decrease in the trans-planar mesophase fraction, as already observed by X-ray analysis. Most probably, in our samples, the fraction of mesophase is organized in very small domains in the amorphous matrix; the UV radiation, attaching the amorphous phase in the neighboring zones of the mesophase domains, causes their instability and determines their reduction. In Figure 3, we can also observe that the melting temperature of the main endotherm shows some variations on increasing of the UV irradiation times. The values, for both series of samples, are reported as a function of the time in Figure 5. The data show that the thermal treatment alone does not change the melting temperature, whereas the UV treatment determines a gradual increase up to 170 h and a decrease for a longer time. These results are consistent with the diffractometric data, which show a growth of the crystallite sizes within the first 200 h of UV exposure and a reversal trend for longer times. The values of crystallinity, obtained using for ΔH_0 the value of 196.6 J/g, are reported as a function of the time in

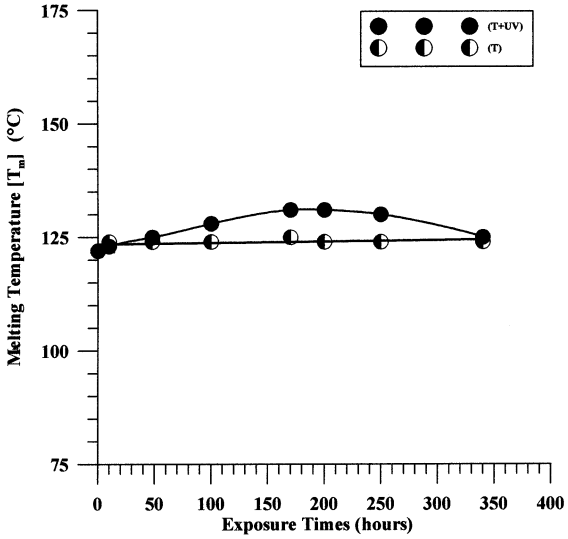

Figure 5. Melting temperatures of the annealed (T) and irradiated (T + UV) samples as a function of the exposure times.

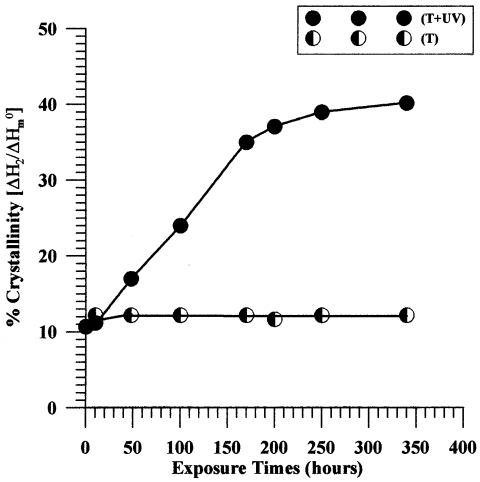

Figure 6. Enthalpic crystallinity of the annealed (T) and irradiated (T + UV) samples as a function of the exposure times.

Figure 6 for both series of samples. The enthalpic crystallinity trend is very similar to that observed by diffractometric analysis, showing a strong increase within the first 170 h and afterward a smaller increase. Also for the enthalpic crystallinity no change is observed for the annealed samples. Another remarkable difference that we can note consists of the broadening of the melting peak in samples irradiated for long times (see Figure 3, sample A340UV). This last datum suggests that the crystallinity increase, for longer irradiation times, occurs with a simultaneous broadening of distribution of the crystal thickness. The dispersity of crystal thickness in each sample can be represented by $I_d = T_m - T_0$, where T_m is the peak melting temperature and T_0 the onset temperature, corresponding to the melting of crystallites with smaller sizes. The onset temperature is determined from the intersection of the slope on the left of the melting endotherm and the baseline. The values of I_d as a function of the time are reported in Figure 7. We can note that the value of I_d is approximately constant for both series of samples up to 170 h; afterward a strong increase is observed for irradiated samples in the range 170−200 h; over 200 h this parameter does not change. It is interesting to note

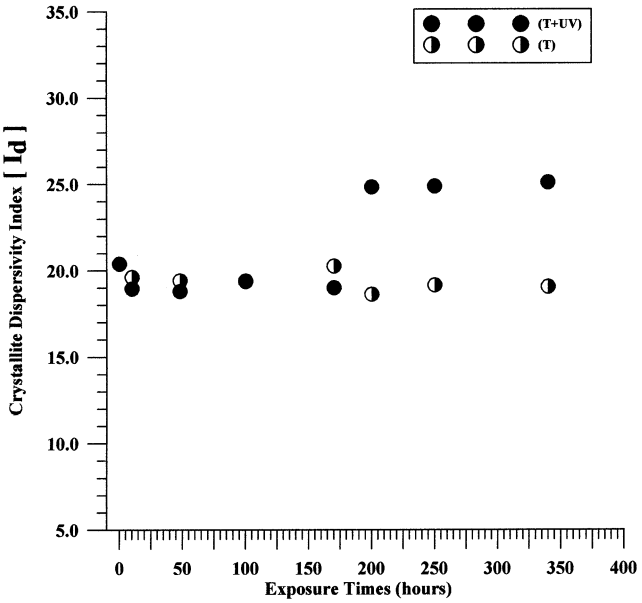

Figure 7. Dispersivity of crystal thickness of the annealed (T) and irradiated (T + UV) samples as a function of the exposure times.

that the strongest increase of crystallinity occurs within the first 170 h, where I_d is approximately constant. Considering the diffractometric data and the trend of the melting temperatures, we deduce that in this range the increase of crystallinity substantially occurs by the growth of preexisting crystals. In the range between 170 and 200 h, new small crystals grow, whose dimensions considerably contribute to the increase of the dispersity. This last phenomenon explains why the profile of the main endotherm is so broadened on the left in the thermograms of samples irradiated for a long time. In fact, in these samples, the morphology is characterized by the coexistence of bigger dimensions crystals, grown on preexisting ones, with populations of defective and small crystals which melt at lower temperatures.

Infrared Analysis. Infrared spectrometry is a powerful tool for studying the UV degradation of the polypropylene because new bands characteristic of the photooxidation products appear in the FT/IR spectra. In particular, two regions[33−35] of the middle infrared spectrum are widely considered; they correspond to the ranges of the O−H stretching modes (3000−3700 cm^{-1}) and the C=O stretching modes (1700−1800 cm^{-1}). In this paper, we have also carefully investigated the interval between 700 and 1300 cm^{-1}, which is the spectral range where the conformational changes can be monitored: in fact, helical and trans-planar bands have been evidenced since the first preparation of the syndiotactic isomer of polypropylene.[36,37]

In Figure 8 we report the spectra in absorbance in the interval 1500−1900 cm^{-1}, in which we can observe the formation and increase of the carbonyl groups of carboxylic acids (∼1712 cm^{-1}), ketones (1718−1722 cm^{-1}), esters (1735−1740 cm^{-1}), and lactones (∼1786 cm^{-1}) as a function of the irradiation time. In the figure, it is also evident the appearance and the increase of a moderate absorption between 1610 and 1660 cm^{-1} due to C=C stretching. From the evolution of the experimental profiles, we can note that no remarkable change is recorded within the first 24 h. The carbonyl groups start to be evident in the spectrum of the sample irradiated 48 h. Between 48 and 100 h, the changes in

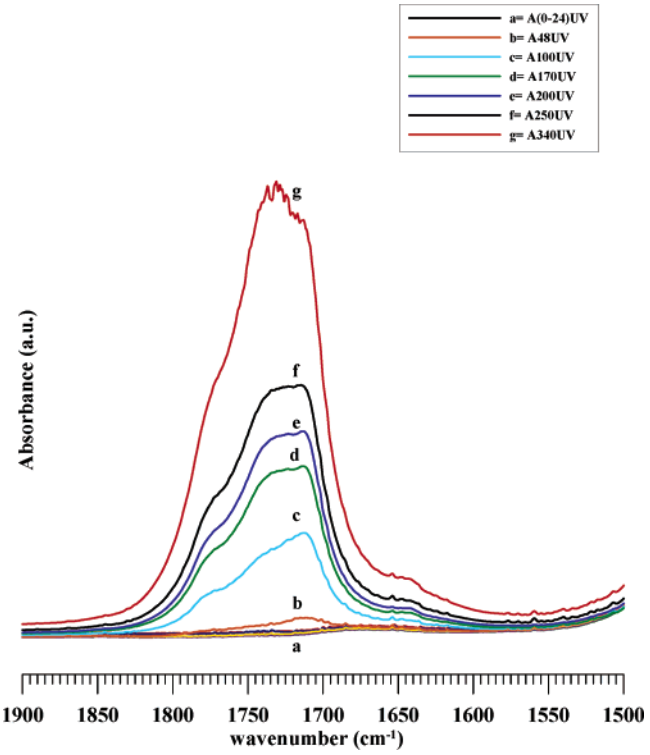

Figure 8. Infrared spectra of samples exposed at increasing UV irradiation times.

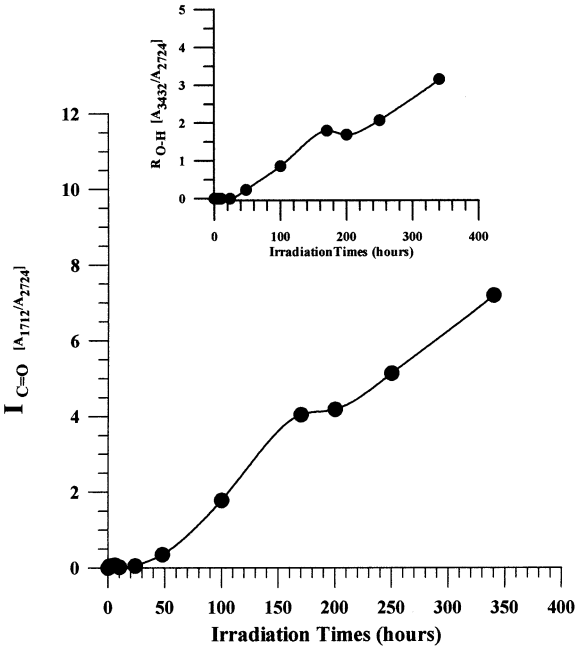

Figure 9. Increase of the absorbance at 1712 cm^{-1} as a function of the irradiation times. Inset: increase of the absorbance at 3432 cm^{-1} as a function of the irradiation times.

the spectra are characterized by the appearance of a broad carbonyl band with a main absorption maximum at 1712 cm^{-1} resulting from the formation of carboxylic acids and three shoulders at 1722, 1735, and 1778 cm^{-1}. The shoulders on the carbonyl band of degraded polyolefins around 1722, 1735, and 1778 cm^{-1} were assigned to the ketones, esters, and lactones, respectively.[38−41] Irradiations for longer times (>100 h) cause modifications of the spectra; the absorption maxima, abovementioned, are still present, but the relative distribution of the peaks is different. Comparing the heights of the different peaks in the sample irradiated 340 h, we can observe that the peak at 1735 cm^{-1} is the most intense. The observed differences in the profiles indicate a more massive formation of ester groups for longer irradiation times. In Figure 9, we show the increase of the band at 1712 cm^{-1} with the irradiation times. For the polyolefins, this band is reported in the literature as carbonyl or aging index. To take into account possible different thickness, we have calculated the carbonyl index normalizing the absorbance of the band at 1712 with the absorbance of the band at 2724 cm^{-1}, obtaining the ratio $I_{CO} = A_{1712}/A_{2724}$. We have chosen the band at 2724 cm^{-1} because, in the sPP, this band is not influenced by the functional groups of the photoproducts and it is independent of the chain conformation. The figure shows an induction period (24 h) before the increase of the carbonyl index. The increase follows three stages: a first faster stage up to 170 h, a plateau, and a slower stage, which starts at 200 h. From these data, we can deduce that the structural and morphological changes due to the radiation cause a more moderate increase in the advanced stage of the photodegradation, when the virgin available amorphous phase for further photooxidative reactions is enormously reduced. It is interesting to note that the slope of the curve is more reduced where also the increase of the crystallinity degree is slower. In fact, both phenomena are related to the effects of the degradation. The plateau in the carbonyl index suggests that, between the two different stages of increase, there is an interval of time where the value of I_{CO} is almost constant. However, the same plateau appears also in the hydroxyl products (see inset in Figure 9). The mechanism commonly invoked in the oxidation process of polyolefins is the attack of free radicals on the polymeric chain. The alkyl radicals generated react with oxygen, giving rise to peroxide radicals and then to hydroperoxides, which decompose producing either ketones or alkoxy radicals and hydroxy radicals, which in turn form other products of photodegradation. The esters are not the primary products of the photooxidation. The more massive formation of esters, which constitute a large proportion of the carbonyl products at longer times of irradiation, is favored when a large concentration of alkoxy radicals and ketones is present in the amorphous matrix. In fact, the mechanism[39] for the formation of esters involves the photolysis of hydroperoxides and the reaction of alkoxy radicals with ketones following the reactions:

$$\mathrm{ROOH} \xrightarrow{h\nu} \mathrm{RO^{\bullet}} + \mathrm{HO^{\bullet}}$$

$$\mathrm{RO^{\bullet}} + \mathrm{P{-}CO{-}P} \rightarrow \mathrm{P{-}COOR} + \mathrm{P^{\bullet}}$$

The plateau that we observe in the I_{CO} and R_{OH} of Figure 9 between 170 and 200 h could be due to a more massive formation of the esters groups because the amorphous phase is very degraded and alkoxy radicals and ketones are very near and therefore under favorable conditions for the above-mentioned reaction. The photolysis has the effect of degrading the hydroperoxides (slight decrease of the hydroxyl absorbance) and the ketones (stopping in the increase of the absorbance at 1720 cm^{-1}); afterward, a strong increase is observed in the formation of esters, which constitute the largest proportion of the carbonyl groups after 200 h of exposure. This result is in accordance with the diffractometric data, which indicate that the increase of the crys-

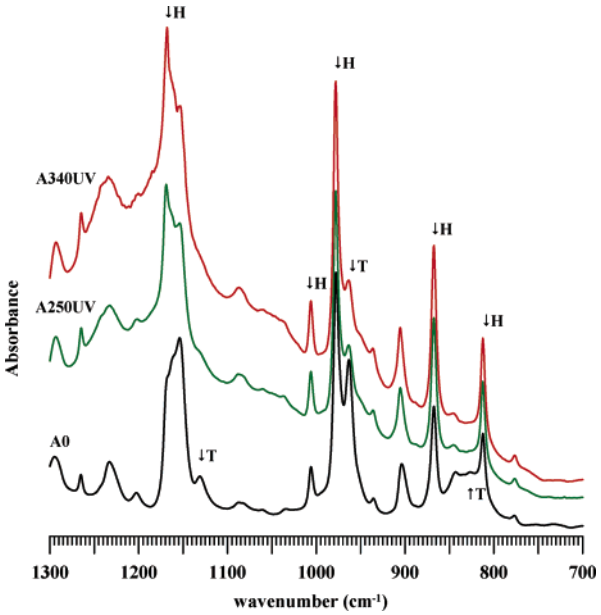

Figure 10. Infrared spectra of A0, A250UV, and A340UV samples.

tallinity degree is less after 200 h of exposure. After this time, the increase cannot occur with the growth of the preexisting crystals, owing to a virgin amorphous phase very reduced also in the bordering zones around the surfaces of the crystallites. When this happens, the lengths of the sequences in the repetitive constitutional units along the chains are very short: the functional groups of the photoproducts are located on adjacent chains, and therefore the reactions, as that which gives the esters, are favored by the proximity of the reactive groups.

In the spectral range, corresponding to the O−H and C=O stretching modes, the spectra in absorbance of samples annealed at 45 °C for increasing times are flat, suggesting that, also for the longest investigated time, the polymer does not undergo photooxidative degradation. These spectra are not reported here because they are equal to that of the starting sample (A0). In Figure 10, the FTIR spectrum in the range (1300−700 cm^{-1}) of the initial sample A0 is put together with spectra of irradiated samples (A250UV and A340UV). We left other spectra out of figure to make it easy to read. For A0 sample, we observe that the bands of the helical form of sPP (denoted with H), appearing at 812, 977, 1005, and 1168 cm^{-1}, are very evident and well developed, confirming that our sample has the chains prevalently in helical conformations. In this spectrum, the presence of long strands of chains in the trans-planar conformation corresponding to the bands at 831, 963, and 1132 cm^{-1} (denoted with T) is also evident, although they show reduced intensity. For the irradiated samples, we can note that all the bands of the helical conformation increase with irradiation time, whereas the bands corresponding to the trans-planar conformation decrease or disappear. In particular, the only band of the trans-planar conformation which remains, although with reduced intensity, in the A340UV sample is the band at 963 cm^{-1}. To understand why the band at 963 cm^{-1} remains also for long irradiated times, we have recorded some spectra FTIR on the sPP melt, with long times of permanence at high temperature (180 °C). The spectrum of the sPP melt has been monitored for 40 min; it has been observed that, after a period of permanence of 5

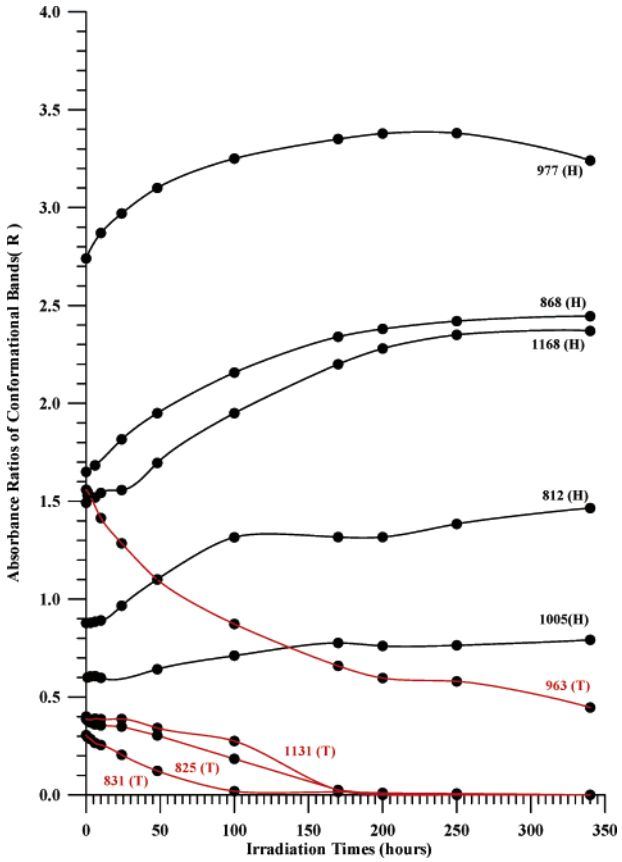

Figure 11. Ratios R for the trans-planar (indicated with T) and helical (indicated with H) bands as a function of the irradiation times.

min at 180 °C, the spectrum does not show any change. The results have shown that small strands of chains adopt a trans-planar conformation also in the melt polymer, where the crystalline or mesomorphic order should be lacking. All the spectra have been recorded in absorbance on films of thickness 70 ± 5 μm. To follow the conformational transformations caused by irradiative treatment, we analyzed the intensity of all the conformational bands as a function of the time. To better study the conformational variations, we take into account the crystallizable amorphous. To this purpose, the contribution of the atactic spectrum was subtracted in all cases. In addition, we normalized the absorbance of these bands with the absorbance of the band at 2724 cm^{-1}, which is independent of the conformation (see before), obtaining the ratio $R = A_{(\text{trans-planar or helical})}/A_{(2724)}$. All the infrared bands, which overlap with other vibrational modes, were decomposed into different components as described in the Experimental Section. Figure 11 shows the ratio R for the trans-planar (indicated with T) and helical (indicated with H) bands as a function of time. The ratio R for the trans-planar bands strongly decreases up to 170 h of the irradiation time. At 170 h, the bands at 831, 825, and 1131 cm^{-1} go to zero, whereas the band at 963 cm^{-1}, after a strong decrease up to 170 h, undergoes only a slight decrease at 340 h. The ratio R for this band, also reaching very small values, does not go to zero. In fact, as previously explained, this band is able to detect very short trans-planar sequences, which remain always in the amorphous phase of the sPP. The trend, for the helical bands, is opposite to that of the trans-planar bands: the strongest increase is observed in the first 170 h, and

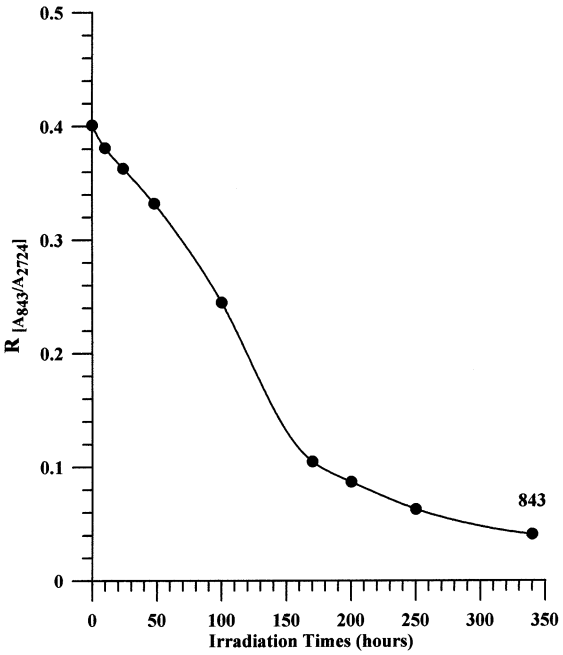

Figure 12. Decrease of the absorbance at 843 cm^{-1} as a function of the irradiation times.

only a slight increase is noticed between 170 and 340 h. From the figure it is evident that the decrease of the trans-planar sequences and the increase of the helical ones, occurring in the same time interval, are correlated events. Figure 12 shows the ratio $R = A_{(843)}/A_{(2724)}$ for the amorphous phase. We have chosen this band to study the changes in the fraction of the amorphous phase after an accurate study of spectra of amorphous polypropylenes. These studies have shown that this band remains in the amorphous polypropylene, and it cannot be assigned to small sequences trans (as the band at 963 cm^{-1}) because it is also present in the atactic polypropylene and amorphous phase of the isotactic polypropylene. Besides, this band was assigned[42] to the vibrational modes corresponding at the CH_2 rock in the amorphous component. Also for the band at 843 cm^{-1}, a rapid decrease is recorded in the first 170 h of irradiation time and a very small decrease between 170 and 340 h. This result is in accordance with all the other discussed data; for example, from diffractometric data we observe an increase of crystalline degree from 17% to 37% in the first 170 h and then only a very small increase up to 340 h. All the data clearly suggest that the increase in the crystalline degree of the samples, recorded in the first 170 h, occurs by a strong reduction of the amorphous phase and of the trans-planar domains which, being very small and arranged in the amorphous matrix, are attached by the UV radiation together with the amorphous phase. Studies are in progress to analyze the effect of UV radiation on the photooxidation of sPP films essentially crystallized in greater and compact domains with chains in the trans-planar conformation. It is interesting to observe that the curve of the amorphous phase (Figure 12) is very similar to the curve of the band at 963 cm^{-1}, which is the most sensitive band to the trans-planar conformations in the amorphous phase. Figure 13 shows the trends for the trans-planar and helical bands of the samples kept at 45 °C for increasing times. From the figure, it is evident that the intensity ratios, for all the bands, do not vary on increasing the permanence time

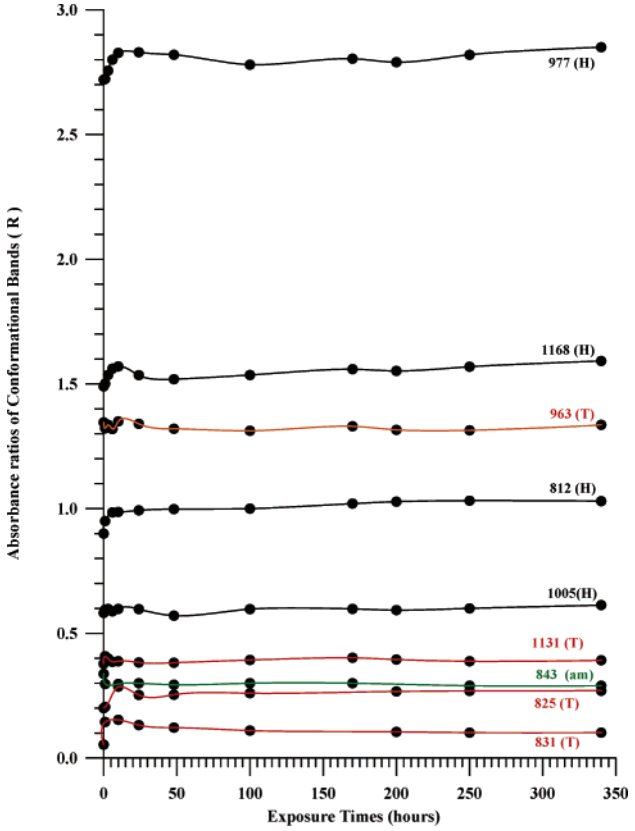

Figure 13. Ratios R for the trans-planar (indicated with T) and helical (indicated with H) bands as a function of the exposure times.

at 45 °C. In fact, we can only note a slight increase (for both the conformations this time) in the first 10 h of treatment. These initial and very small phase reorganizations, which realize by an increase in the conformational order of the trans-planar and helical chains, could be due to an accelerated physical aging of the amorphous phase.

Comparing the data of the Figures 11 and 13, we can conclude that also the spectroscopic data indicate that the strong structural and morphological modifications are to be ascribed to the effect of UV radiation.

Conclusive Remarks

The results of the present study evidence the effect of the UV radiation on the morphology of sPP samples obtained quenching the sPP melt at 25 °C. This procedure allows us to get films in the most usual form I, with the chains in helical conformation. In addition, a fraction of chains in trans-planar conformation is also formed and organized in small domains in the amorphous matrix. The radiative treatment determines a complex structural and morphological reorganization in terms of crystallinity, crystal dimensions, and fraction of trans-planar mesophase. This reorganization was not found in the thermally treated samples, which undergo only a very small increase of the trans-planar and helical conformational order within the first hours of treatment. The cause of the strong changes is the chains scission due to the photooxidation. The chains scission determines a shortening of the amorphous chains, making them more mobile and free to crystallize further in the more stable helical form I. The increase in crystallinity degree in the first 170 h occurs by the growth of the crystal dimensions in the direction

perpendicular to the (200) planes, whereas no appreciable changes are noted for the direction perpendicular to the (010) planes. This result indicates a different ability, in the two crystallographic directions, of lamellar crystals with chains in helical conformations, to host defects during the crystallization process induced by the UV radiation. The increase of the crystallinity is reduced after 170 h of irradiance. This more reduced increase is realized by the formation of new small crystals in the amorphous matrix. The increase in the crystallinity degree within the first 170 h occurs by a strong increase of the helicoidal conformational order and a strong reduction of the amorphous and trans-planar domains. The decrease of the trans-planar sequences and the increase of the helical ones are correlated events. Both the effects are correlated to transformations, which convert one phase into the other. The similarity in the trend of the FTIR curves of the amorphous phase and the trans-planar bands very probably indicates that the trans-planar domains are very small and finely distributed in the amorphous matrix, and therefore they are consumed with the same kinetics of the amorphous component.

Acknowledgment. This work was supported by MIUR-Italia (PRIN 2002).

References and Notes

(1) Ewen, J. A.; Jones, J. A.; Razavi, A.; Ferrara, J. D. *J. Am. Chem. Soc.* **1988**, *101*, 6255.
(2) Longo, P.; Proto, A.; Grassi, A.; Ammendola, P. *Macromolecules* **1992**, *24*, 462.
(3) Grisi, F.; Longo, P.; Zambelli, A.; Ewen, J. A. *J. Mol. Catal. A: Chem.* **1999**, *140*, 225.
(4) D'Aniello, C.; Guadagno, L.; Naddeo, C.; Vittoria, V. *Macromol. Rapid Commun.* **2000**, *21*, 104.
(5) D'Aniello, C.; Guadagno, L.; Naddeo, C.; Vittoria, V. *Proceeding XV° Convegno Italiano di Scienza e Tecnologia delle Macromolecole A.I.M.* Trieste-Italia, 24−27 Sept 2001.
(6) Guadagno, L.; D'Aniello, C.; Naddeo, C.; Vittoria, V. *Macromolecules* **2001**, *34*, 2521.
(7) Guadagno, L.; D'Aniello, C.; Naddeo, C.; Vittoria, V.; Meille, S. V. *Macromolecules* **2002**, *35*, 3921.
(8) Guadagno, L.; D'Aniello, C.; Naddeo, C.; Vittoria, V.; Meille, S. V. *Macromolecules* **2004**, *37*, 5977.
(9) Lotz, B.; Lovinger, A. J.; Cais, R. E. *Macromolecules* **1988**, *21*, 2375.
(10) De Rosa, C.; Corradini, P. *Macromolecules* **1993**, *26*, 5711.
(11) Chatani, Y.; Maruyama, H.; Noguchi, K.; Asanuma, T.; Shiomura, T. *J. Polym. Sci., Part C* **1990**, *28*, 393.
(12) Chatani, Y.; Maruyama, H.; Asanuma, T.; Shiomura, T. *J. Polym. Sci., Part B: Polym. Phys. Ed.* **1991**, *29*, 1649.
(13) Lovinger, A. J.; Lotz, B.; Cais, R. E. *Polymer* **1990**, *31*, 2253.
(14) Lovinger, A. J.; Davis, D. D.; Lotz, B. *Macromolecules* **1991**, *24*, 552.
(15) Lovinger, A. J.; Lotz, B.; Davis, D. D.; Padden, F. *Macromolecules* **1993**, *26*, 3494.
(16) De Rosa, C.; Auriemma, F.; Vinti, V. *Macromolecules* **1997**, *30*, 4137.
(17) Nakaoki, T.; Ohira, Y.; Hayashi, H.; Horii, F. *Macromolecules* **1998**, *31*, 2705.
(18) Vittoria, V.; Guadagno, L.; Comotti, A.; Simonutti, R.; Auriemma, F.; De Rosa, C. *Macromolecules* **2000**, *33*, 6200.
(19) Guadagno, L.; D'Aniello, C.; Naddeo, C.; Vittoria, V. *Macromolecules* **2000**, *33*, 6030.
(20) Yoshino, K.; et al. *IEEE Trans. Dielectr. Electr. Insul.* **1996**, *3*, 331.
(21) Kim, D. W.; Yoshino, K. *J. Phys. D: Appl. Phys.* **2000**, *33*, 464.
(22) Kohalmy, S.; Banhegyi, G.; Kimura, H.; Tanaka, T. High Voltage Engineering Symposium; *Conference Publication IEE No. 467,* 1999.
(23) Natta, G.; Corradini, P.; Cesari, M. R. *Acc. Lincei* **1957**, *58*, 22, 11.
(24) Guadagno, L.; D'Aniello, Gorrasi, G.; C.; Naddeo, C.; Vittoria, V. *J. Macromol. Sci., Phys.* **2002**, *B41*, 289.
(25) Tadokoro, H. *Structure of Crystalline Polymers*; John Wiley: New York, 1978.
(26) Guadagno, L.; D'Arienzo, L.; Vittoria, V.; Longo, P.; Romano, G. *J. Macromol. Sci., Phys.* **2000**, *B39*, 425.
(27) Schwartz, J.; Stronz, M.; Bonnet, M.; Petermann, M. *J. Colloid Polym. Sci.* **2001**, *506*, 279.
(28) Lacks, D. *Macromolecules* **1996**, *29*, 1849.
(29) Palmo, K.; Krimm, S. *Macromolecules* **1996**, *29*, 8549.
(30) Uehara, H.; Yamazaki, Y.; Kanamoto, T. *Polymer* **1996**, *37*, 57.
(31) Guadagno, L.; D'Aniello, C.; Naddeo, C.; Vittoria, V.; Meille, S. V. *Macromolecules* **2003**, *36*, 6756.
(32) Guadagno, L.; D'Aniello, C.; Naddeo, C.; Vittoria, V. *J. Macromol. Sci., Phys.* **2004**, *B43*, 989.
(33) Hamid, S. H.; Amin, M. B.; Maadhah, A. G. *Handbook of Polymer Degradation*, 1st ed.; Marcel Dekker: New York, 1992.
(34) Lacoste, J.; Carlsson, D. J. *J. Polym. Sci., Part A* **1992**, *30*, 493.
(35) Lacoste, J.; Vallilant, D.; Carlsson, D. J. *J. Polym. Sci., Part A* **1993**, *31*, 715.
(36) Corradini, P.; Natta, G.; Ganis, P.; Temussi, P. A. *J. Polym. Sci.* **1967**, *16*, 2477.
(37) Natta, G.; Corradini, P.; Ganis, P. *Makromol. Chem.* **1960**, *39*, 238.
(38) Swern, D.; Witnauer, L. P.; Eddy, C. R.; Parker, W. E. *J. Am. Chem. Soc.* **1955**, *77*, 5537.
(39) Geuskens, G.; Kabamba, M. S. *Polym. Degrad. Stab.* **1982**, *4*, 69.
(40) Adams, J. H. *J. Polym. Sci., Part A* **1970**, *8*, 1077.
(41) Lacoste, J.; Arnaud, R.; Singh, R. P.; Lemaire, J. *J. Makromol. Chem.* **1988**, *189*, 651.
(42) Nakaoki, T.; Yamanaka, T.; Ohira, Y.; Horii, F. *Macromolecules* **2000**, *33*, 2718.

MA040129J